

# Neural-Network based Swing-up and Stabilization Control of Rotary Inverted Pendulum Systems <sup>\*</sup>

DongBeom Kim <sup>\*</sup> Ngo Phong Nguyen <sup>\*\*</sup> Jun Moon <sup>\*</sup>

<sup>\*</sup> Department of Electrical Engineering, Hanyang University, Seoul, South Korea (e-mails: {rlaehdqa, junmoon}@hanyang.ac.kr)

<sup>\*\*</sup> Department of Mechanical Engineering, Ulsan National Institute of Science and Technology (UNIST), Ulsan, South Korea (email: ngophong@unist.ac.kr)

**Abstract:** We propose the neural-network based control (NNC) approach for rotary inverted pendulum (RIP). The control structure for RIP consists of two phases: (i) swing-up phase, which drives the pendulum up towards the desired upright position; and (ii) stabilization phase, which enables the pendulum to keep the desired upright position. In our paper, the swing-up controller is designed based on energy control approach with feedback linearization technique, where the corresponding control gain  $K_{EC}$  is determined by the proposed NNC. Next, the stabilization controller is designed based on modified super-twisting sliding-mode control (MSTSMC) algorithm, which requires to design a new sliding surface in order to achieve the asymptotic stability of RIP. Similar to the swing-up phase, the control gain  $K_{SS}$  of the MSTSMC is determined intelligently by the proposed NNC. In fact, the proposed NNC allows to select  $K_{EC}$  and  $K_{SS}$  adaptively based on the operation of RIP. Finally, we provide the experimental comparisons between the proposed NNC and the control system of RIP without the neural-network framework. Through the experimental results, we show that by the NNC, the proposed control system of RIP provides the better swing-up and stabilization performances.

Copyright © 2023 The Authors. This is an open access article under the CC BY-NC-ND license (<https://creativecommons.org/licenses/by-nc-nd/4.0/>)

**Keywords:** Energy control, Feedback linearization, Neural network, Rotary inverted pendulum, Super-twisting sliding-mode control, Swing-up and stabilization control.

## 1. INTRODUCTION

Rotary inverted pendulum (RIP) systems have been applied into numerous fields of engineering (see Hamza et al. (2019); Nghi et al. (2022); Dolatabad et al. (2022)). Hence, the improvement of RIP control performance can be regarded as an important topic in the area of control theory and its applications. RIP consists of rotary arm and pendulum parts. In particular, the arm part rotates in horizontal plane, whereas the pendulum part, which is connected at the end of the rotary arm, fully rotates in vertical plane. As a result, RIP belongs to a class of two-degree-of-freedom systems. Note also that RIP is an under-actuated system, since its control input is only applied to the rotary arm.

In general, the control structure for RIP includes two phases: (i) swing-up phase, which drives the pendulum up towards the desired upright position; and (ii) stabilization phase, which enables the pendulum to keep the desired upright position. Note that the control problem of RIP is a challenging task. On the one hand, RIP is an under-

actuated system and its dynamic model is highly nonlinear. On the other hand, the equilibrium point of RIP in the upright position is generally unstable. Hence, various control approaches have been proposed to overcome such challenges. Interested readers are referred to the work of Hamza et al. (2019); Nghi et al. (2022); Dolatabad et al. (2022) for comprehensive reviews on the control methods for RIP. Note that in most of previous approaches, for the desirable performance of RIP, the trial and error process for parameter tuning is required, which is a time-consuming procedure. Hence, it is essential to develop the intelligent approach to select optimal swing-up and stabilization control gains, which reduces the implementation effort and further enhances the performance of RIP.

In this paper, we propose the NNC approach for RIP. First, the swing-up controller is designed based on the energy approach with feedback linearization technique, where the corresponding control gain  $K_{EC}$  is determined intelligently by the proposed NNC. Next, the stabilization controller is designed based on the MSTSMC, which requires to design a new (coupled) sliding surface in order to achieve the asymptotic stability of RIP. Similar to the swing-up phase, the control gain  $K_{SS}$  of the MSTSMC is determined intelligently by the proposed NNC. In brief, the proposed NNC allows to select  $K_{EC}$  and  $K_{SS}$  adaptively based on the operation of RIP. We finally demonstrate the effectiveness of the proposed NNC via extensive experimental results.

<sup>\*</sup> This work was supported in part by the Technology Innovation Program (20018112) funded by the Ministry of Trade, Industry and Energy (MOTIE, Korea), in part by the National Research Foundation of Korea (NRF) Grant funded by the Ministry of Science and ICT, South Korea (NRF-2021R1A2C2094350), and in part by Institute of Information & Communications Technology Planning and Evaluation (IITP) grant funded by the Korea government (MSIT) (No.2020-0-01373).

## 2. DYNAMIC MODELING FOR RIP

Based on the Euler-Lagrange approach, the dynamic model of RIP is given as follows (Hamza et al. (2019)):

$$\begin{aligned} A_1\ddot{\theta} - A_2\ddot{\alpha} + A_3\dot{\theta}\dot{\alpha} + A_4\dot{\alpha}^2 &= \tau \\ B_1\ddot{\alpha} - B_2\dot{\theta}^2 - B_3\dot{\theta}^2 - B_4 &= 0, \end{aligned} \quad (1)$$

where

$$\begin{aligned} A_1 &= m_p L_r^2 + J_r + \frac{1}{4} m_p L_p^2 \sin^2(\alpha), \quad A_2 = \frac{1}{2} m_p L_p L_r \cos(\alpha) \\ A_3 &= \frac{1}{2} m_p L_p^2 \sin(\alpha) \cos(\alpha), \quad A_4 = \frac{1}{2} m_p L_p L_r \sin(\alpha) \\ B_1 &= J_p + \frac{1}{4} m_p L_p^2, \quad B_2 = \frac{1}{2} m_p L_p L_r \cos(\alpha) \\ B_3 &= \frac{1}{4} m_p L_p^2 \sin(\alpha) \cos(\alpha), \quad B_4 = \frac{1}{2} m_p L_p g \sin(\alpha). \end{aligned}$$

with  $m_p$  represents the mass of the pendulum;  $L_r$  and  $L_p$  express the total length of the arm and pendulum, respectively;  $J_r$  represents the moment of inertia of the arm;  $J_p$  is the moment of inertia of the pendulum;  $\tau$  is the control input; and  $\theta$  and  $\alpha$  denote the rotary arm and pendulum angles, respectively.

## 3. NEURAL-NETWORK BASED CONTROL FOR RIP

### 3.1 Swing-up Control of RIP

For the swing-up control, we utilize the energy control approach with feedback linearization technique, in which the swing-up gain  $K_{EC}$  is an important design parameter. Besides, we provide the design methodology to select  $K_{EC}$  optimally via the proposed NNC.

*Energy Control with Feedback Linearization:* From (1), we first rewrite the  $\ddot{\theta}$ -dynamics in the following form:

$$\ddot{\theta} = f_1(\alpha)\tau + f_2(\alpha, \dot{\alpha}, \dot{\theta}), \quad (2)$$

where the definitions of  $f_1(\alpha)$  and  $f_2(\alpha, \dot{\alpha}, \dot{\theta})$  can be found in Nguyen et al. (2021). Then, by using the feedback linearization technique (see Khalil (2001)), the control law, which uses  $\ddot{\theta}$  as a new control input, can be derived. In particular, we define the new control input  $\tau_{new} = \ddot{\theta}$ . In that context, the control input  $\tau$  in (2) is defined as follows:

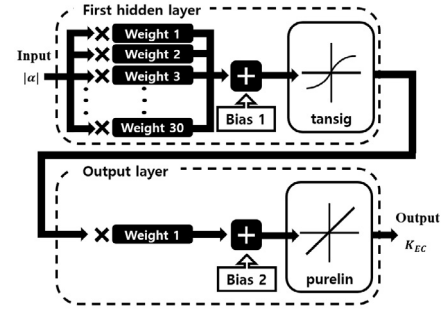
$$\tau := \tau_{sw} = \frac{1}{f_1(\alpha)}[\tau_{new} - f_2(\alpha, \dot{\alpha}, \dot{\theta})], \quad (3)$$

where  $\tau_{sw}$  is the control input torque of RIP when the swing-up controller is applied, and  $\tau_{new}$  is the energy-based control law, which is given by

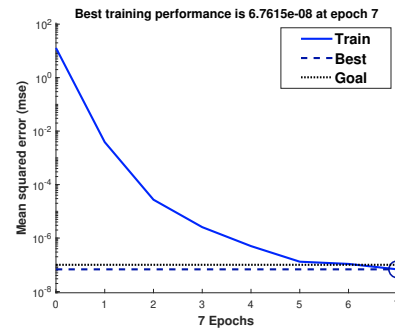
$$\tau_{new} = -\frac{2}{m_p L_p L_r} K_{EC} \text{sign}((E - E_d)\dot{\alpha} \cos(\alpha)), \quad (4)$$

where  $K_{EC}$  is a positive control gain,  $E$  denotes the energy of the uncontrolled pendulum, i.e.,  $E = \frac{1}{2}(J_p + \frac{1}{4}m_p L_p^2)\dot{\alpha}^2 + \frac{1}{2}m_p g L_p \cos(\alpha)$ , and  $E_d$  represents the energy of the pendulum at the upright position, i.e.,  $E_d = \frac{1}{2}m_p g L_p$ .

*Neural-Network Control for the Energy Controller:* As shown in (4),  $K_{EC}$  can be any positive constant. From the mathematical verification and numerical simulations, we notice that as  $K_{EC}$  gets bigger, the time to change from the swing-up controller to the stabilization controller,



(a) The NNC scheme for swing up.



(b) Mean squared error of energy control.

Fig. 1. The proposed NNC for the energy controller.

denoted by  $T_{sw}$ , gets shorter (see Nguyen et al. (2021) for relevant discussions). However, the large  $K_{EC}$  causes the excessive input torque. This implies that RIP might swing over the switching criterion or be fully rotated. On the other hand, the small  $K_{EC}$  induces stable but slow motion. Similar to the case with the large  $K_{EC}$ , several problems such as taking too much time to achieve the goal position or not able to achieve the goal position might be happened.

The above discussion implies that we need to find an appropriate  $K_{EC}$  for the swing-up controller. Hence, we propose the neural-network control (NNC) scheme. The detailed architecture of the proposed NNC for energy controller is as follows. First, we generate the dataset for the NNC for learning by using the fuzzy logic scheme. To do this, we design the fuzzy rule for the energy controller by identifying appropriate input and output relationship. Second, based on these datasets, we design the NNC for energy control, which is feedforward, and has 1 hidden layer (Layer 2) and output layer (Layer 4). The NNC of swing-up has 30 nodes in its Layer 2. Each input of NNC passes the nodes and is summed with bias. Then, this value passes the first active function, which has the tansig function structure. The output of first active functions is the input of Layer 3, which passes through nodes and is summed with another bias Layer 2. The result of this process is input to linear active function and outputs the gain (i.e.,  $K_{EC}$ ). The detailed architecture of the proposed NNC for swing-up control is given in Fig. 1. Besides, Fig. 1(b) shows the mean-square error between the input dataset and the proposed NNC with the target learning error of  $10^{-7}$ . Note that as can be seen from Fig. 1(b), the difference between the designed network and the input dataset is almost zero as epochs increase. In fact, the mean-square error decreases to a small value within 7 epochs.

### 3.2 Stabilization Control of RIP

If RIP reaches the switching criterion (i.e.,  $\frac{\pi}{15}$ ), the stabilization controller should be applied in order to stabilize RIP. In this subsection, we design the NNC-based modified super-twisting sliding mode controller (MSTSMC), where we propose the neural-network architecture to determine gain  $K_{SS}$  of MSTSMC intelligently.

**Control Law Design for MSTSMC:** As in Nguyen et al. (2020), we first define the new (coupled) sliding surface as

$$s = k_\theta \dot{\theta} + k_\alpha \dot{\alpha} + \lambda_\theta \theta + \lambda_\alpha \alpha, \quad (5)$$

where  $k_\theta$ ,  $k_\alpha$ ,  $\lambda_\theta$ ,  $\lambda_\alpha$  are sliding surface gains. Note that from (1) and (2), the  $\ddot{\alpha}$ -dynamics can be rewritten in the following form:

$$\ddot{\alpha} = f_3(\alpha)\tau + f_4(\alpha, \dot{\alpha}, \dot{\theta}), \quad (6)$$

where the definitions of  $f_3(\alpha)$  and  $f_4(\alpha, \dot{\alpha}, \dot{\theta})$  can be found in Nguyen et al. (2021). Then, MSTSMC algorithm with control gain  $K_{SS}$  is defined as

$$\begin{aligned} \tau := \tau_{st} &= \frac{1}{k_\theta f_1(\alpha) + k_\alpha f_3(\alpha)} [k_\theta f_2(\alpha, \dot{\alpha}, \dot{\theta}) \\ &\quad + k_\alpha f_4(\alpha, \dot{\alpha}, \dot{\theta}) + \lambda_\theta \dot{\theta} + \lambda_\alpha \dot{\alpha} + k_1(t)\varphi_1(s) - z] \\ \dot{z} &= -k_2(t)\varphi_2(s), \end{aligned} \quad (7)$$

where  $\varphi_1(s)$ ,  $\varphi_2(s)$  are given by

$$\varphi_1(s) = |s|^{\frac{1}{2}} \text{sign}(s) + k_3 s \quad (8)$$

$$\varphi_2(s) = \frac{1}{2} \text{sign}(s) + \frac{3}{2} k_3 |s|^{\frac{1}{2}} \text{sign}(s) + k_3^2 s.$$

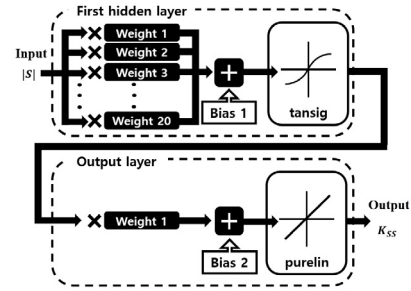
Note that  $k_1$  and  $k_2$  are defined as follows:

$$k_1(t) = \frac{1}{2\beta_0} [4\alpha_0(\beta_0 + 4\alpha_0^2) + 2\alpha_0 + K_{SS}] \quad (9)$$

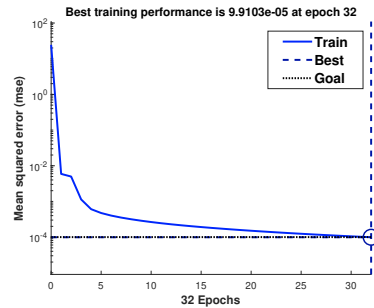
$$k_2(t) = \beta_0 + 4\alpha_0^2 + 2\alpha_0 k_1(t),$$

where  $\alpha_0$  and  $\beta_0$  are positive.  $K_{SS}$  is the gain of MSTSMC that will be defined by the proposed NNC for stabilization below. Note that  $k_\theta$  and  $k_\alpha$  are must satisfy the condition  $k_\theta f_1(\alpha) + k_\alpha f_3(\alpha) \neq 0$  during the stabilization of RIP. For the process of selecting values in the experiment, we refer a discussion in Nguyen et al. (2020, Remark 2).

**Neural-Network Control for MSTSMC:** Thanks to the generation of continuous control signal, the MSTSMC can alleviate but cannot (totally) eliminate the chattering phenomenon. Therefore, it is essential to design the NNC to further reduce the chattering and enhances the performance of the closed-loop system. As discussed in Nguyen et al. (2020), there are differences in the sliding variable dynamics with the variation of  $K_{SS}$ . In particular, a large value of  $K_{SS}$  might drive the sliding variable  $s$  to go zero quickly, with the possible side-effect of large chattering. The small  $K_{SS}$ , which results in a small chattering, will force  $s$  converging to zero slowly. This implies that it is important to choose an appropriate value of  $K_{SS}$  intelligently. In that context, we design the algorithm such that as  $|s|$  is large, the large  $K_{SS}$  is chosen; otherwise, a small value of  $K_{SS}$  is selected. Hence, we utilize  $|s|$  as an input,  $K_{SS}$  as an output. The design of the proposed NNC for the stabilization control is similar to the case of the swing-up control, which is not repeated here due the space limitation. Note that the detailed architecture of the proposed NNC for stabilization control is given in Fig. 2.



(a) The NNC scheme for stabilization.



(b) Mean squared error of stabilization.

Fig. 2. The proposed NNC for the stabilization controller.

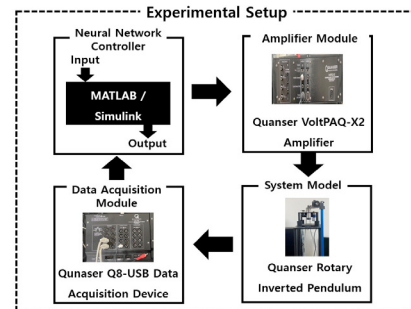


Fig. 3. Experimental setup of RIP control system.

Besides, Fig. 2(b) shows the mean-square error between the input dataset and the proposed NNC with the target learning error of  $10^{-4}$ . As shown in Fig. 2(b), the difference between the designed network and the input dataset is almost zero as epochs increase. In fact, the mean-square error decreases to a small value within 32 epochs.<sup>1</sup>

## 4. EXPERIMENTAL RESULTS

### 4.1 Experiment Set-up

The experiment configuration consists of hardware and software parts. The hardware part includes RIP mounted on the Quanser SRV02 unit, the VoltPAQ-X2 amplifier, and the Q8-USB DAQ control board, all from Quanser company. The software part includes the proposed NNC and the real-time control environment in MATLAB/Simulink provided by Quanser. The structure of the experimental platform is shown in Fig. 3.

<sup>1</sup> Note that the stability of RIP system under the proposed NNC in the swing-up and stabilization phases can be shown by applying the same procedure discussed in Nguyen et al. (2021) that is omitted here due to the space limitation.

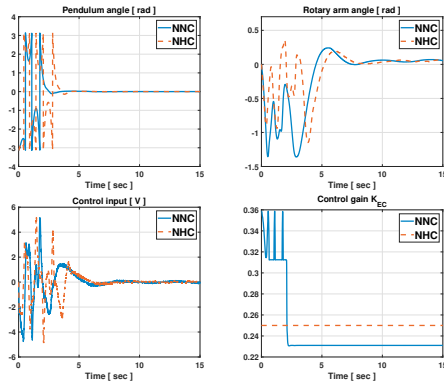


Fig. 4. The experimental results of the proposed NNC for swing-up control (Group 1).

Table 1. Comparison of NNC and NHC

	$T_{sw}$ (sec)	A.C.E. (V)	$T_{st}$ (sec)	Avg. 1 (rad)	Avg. 2 (rad)
NHC	3.172	2.17	8.612	0.0041	0.0710
NNC	<b>2.756</b>	<b>2.21</b>	<b>6.824</b>	<b>0.0014</b>	<b>0.0082</b>

For verification, we conduct the following two different experiment groups: (i) in Group 1, we show the superiority of the swing-up controller in proposed NNC by comparing it with the swing-up method in the nonlinear hybrid controller (NHC) in Nguyen et al. (2021); and (ii) in Group 2, we show the superiority of the stabilization controller in the proposed NNC by comparing it with the stabilization method in the NHC. Besides, we utilize the following two control indices for comparison purposes: (i)  $T_{sw}$ : time to change from swing-up to stabilization within  $|\alpha| \leq 0.5$  (rad); and (ii)  $T_{st}$ : time to satisfy the stabilization condition of  $|\alpha| \leq 0.002$  (rad).

#### 4.2 Group 1

The values of the control parameters of the proposed NNC are selected as  $k_\theta = -0.1$ ,  $k_\alpha = 0.2$ ,  $\lambda_\theta = -0.1$ ,  $\lambda_\alpha = 3.1$  and  $\alpha_0 = 0.25$ ,  $\beta_0 = 0.1$ ,  $k_3 = 0.5$ . Besides, for a fair comparison, the values of the control parameters of the NHC are selected properly as in Nguyen et al. (2021). As shown in Fig. 4, both approaches can drive the pendulum to the switching criterion to change the operation phase from swing-up to stabilization. In Table 1, A.C.E. is the average of the absolute value of the control input. From Table 1 and Fig. 4, we can observe that the proposed NNC requires a shorter time than that of the NHC for swing-up, while both approaches induce a similar control effort. Therefore, we can conclude that the proposed NNC shows the better swing-up performance compared with the NHC.

#### 4.3 Group 2

In this experiment, we use the same values of the control parameters as in Group 1 for both approaches. In Table 1, Avg. 1 and Avg. 2 are the average values of the arm angle  $\alpha$  and the pendulum angle  $\theta$  from 7.5 (sec) to 15 (sec), respectively. From Fig. 5 and Table 1, we can observe

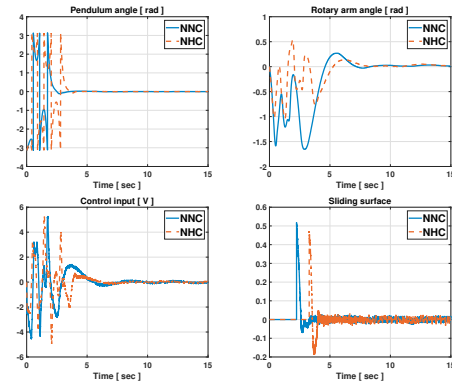


Fig. 5. The experimental results of the proposed NNC for stabilization control (Group 2).

that the proposed NNC shows the better stabilization performance than the NHC. Besides, the stabilization time  $T_{st}$  with the NNC is shorter than that of the NHC.

In brief, in view of the given results, we can state that the proposed NNC shows the better RIP control performance compared with that of the NHC in Nguyen et al. (2021).<sup>2</sup>

## 5. CONCLUSIONS

In this paper, we have proposed the NNC-based control system for RIP to improve its swing-up and stabilization performances. By the proposed NNC, it is possible to choose swing-up and stabilization control gains intelligently through operation of RIP. Through various experimental results, we have demonstrated the effectiveness of the proposed NNC. One possible future research direction is to apply the NNC to other applications such as autonomous driving systems and quadrotors.

## REFERENCES

- Dolatabad, M.R., Pasharavesh, A., and Khayyat, A.A.A. (2022). Analytical and experimental analyses of nonlinear vibrations in a rotary inverted pendulum. *Nonlinear Dynamics*, 107(3), 1887–1902.
- Hamza, M.F., Yap, H.J., Choudhury, I.A., Isa, A.I., Zimit, A.Y., and Kumbasar, T. (2019). Current development on using rotary inverted pendulum as a benchmark for testing linear and nonlinear control algorithms. *Mechanical Systems and Signal Processing*, 116, 347–369.
- Khalil, H. (2001). *Nonlinear Systems*. Pearson.
- Nghi, H.V., Nhien, D.P., and Ba, D.X. (2022). A LQR neural network control approach for fast stabilizing rotary inverted pendulums. *International Journal of Precision Engineering and Manufacturing*, 23(1), 45–56.
- Nguyen, N.P., Oh, H., Kim, Y., and Moon, J. (2021). A nonlinear hybrid controller for swinging-up and stabilizing the rotary inverted pendulum. *Nonlinear Dynamics*, 104(2), 1117–1137.
- Nguyen, N.P., Oh, H., Kim, Y., Moon, J., Yang, J., and Chen, W.H. (2020). Fuzzy-based super-twisting sliding mode stabilization control for under-actuated rotary inverted pendulum systems. *IEEE Access*, 8, 185079–185092.

<sup>2</sup> The experiment video is available at <https://youtu.be/nMbuDxR-XHU>